PERGAMON

International Journal of Heat and Mass Transfer 43 (2000) 1563–1572

International Journal of HEAT and MASS TRANSFER

www.elsevier.com/locate/ijhmt

Mixed convection of micropolar fluids in a cavity

Tsan-Hui Hsu*, Sheng-Gwo Wang

Department of Mechanical Engineering, National Kaohsiung Institute of Technology, Kaohsiung 80782, Taiwan

Received 5 February 1999; received in revised form 15 July 1999

Abstract

A numerical study of the laminar mixed convection of micropolar fluids in a square cavity with localized heat source is presented. The flow in the cavity includes the externally induced stream at ambient temperature and the free flow induced by heat source. The transport equations of vorticity, angular momentum, and energy are solved with the aid of the cubic spline collocation method. The computation is carried out for wide ranges of Reynolds number, Grashof number, and various material parameters associated with the micropolar fluids. Emphasis is aimed at the significant features displayed by the micropolar fluids. The results indicate that both the flow and the thermal fields depend on the vortex viscosity and spin gradient viscosity to a large extent. The heat transfer coefficient of micropolar fluids is found to be smaller than that of Newtonian fluids.

1. Introduction

A number of studies on the convective heat transfer in enclosure, such as solar collection systems, room ventilation, and electronic circuitry have been extensively reported regarding the cooling process [1–3]. Recently, considerable attention has turned to mixed convection problems owing to many practical applications including cooling of electronic equipments and devices [4,5]. In an enclosure, the interaction between the external forced stream and the buoyancy driven flow induced by the increasing high heat flux from electronic modules leads to the possibility of complex flows. Therefore it is important to understand the heat transfer characteristics of mixed convection in an enclosure.

Mixed convection flow and heat transfer have been studied for inclined channels with discrete heat sources [6,7]. It was found in [6] that the best performance in heat transfer is obtained when the channel is in a vertical location. In [7], it pointed out that the normalized Nusselt number is a decreasing function of the Reynolds number and an increasing function of the inclined angle. Papanicolaou and Jaluria [8,9] studied mixed convection from an isolated heat source in a rectangular enclosure. They indicated that flow patterns generally consist of high- or low-velocity recirculating cells due to buoyancy forces generated by the heat source. In addition, the effect of the thermal conductivity of the cavity walls on the heat transfer phenomena was investigated in Ref. [9]. A later investigation [10] further presented turbulent flow in a cavity by k–ε model. Turbulent results were obtained for $Re = 1000$ and 2000 in the ranges of $Gr = 5 \times 10^7 - 5 \times 10^8$. A detailed study of mixed convection in a partially divided rectangular enclosure was presented by Hsu et al. [11]. It was observed that the heat transfer coefficient decreases rather rapidly as the height of the partition is more than about half of the total height of the enclosure.

* Corresponding author. Tel.: +886-73814526; fax: +886-73838435.

0017-9310/00/$ - see front matter
PII: S0017-9310(99)00242-2

Nomenclature

A	height of the inflow and outflow openings
B	material parameter [$= A^2/j$]
Gr	Grashof number [$= g\beta\Delta T A^3/\nu^2$]
H	height of the cavity
j	microinertia per unit mass
k	thermal conductivity
k_v	vortex viscosity
Nu	Nusselt number
Pr	Prandtl number [$= \nu/\alpha$]
q''	heat flux per unit area of the source
Re	Reynolds number [$= v_i A/\nu$]
T	temperature
u, v	horizontal and vertical velocity components, respectively
U, V	dimensionless velocity components [$U = u/v_i$, $V = v/v_i$]
v_i	inlet flow velocity
W	width of the cavity
x, y	Cartesian coordinates
X, Y	dimensionless Cartesian coordinates [$X = x/A$, $Y = y/A$]
α	thermal diffusivity of the fluid
β	coefficient of thermal expansion
γ	spin gradient viscosity
σ	angular velocity component
υ	dimensionless microrotation [$= \sigma A/v_i$]
Δ	material parameter [$= k_v/\mu$]
λ	material parameter [$= \gamma/(j\mu)$]
ΔT	temperature scale [$= q'' A/k$]
θ	dimensionless temperature [$= (T - T_i)/\Delta T$]
ν	kinematic viscosity
ψ	stream function
Ψ	dimensionless stream function [$= \psi/(v_i A)$]
ω	vorticity
Ω	dimensionless vorticity [$= \omega A/v_i$]
η	buoyancy parameter [$= Gr/Re^2$]

Subscripts

i	inflow
o	outflow
s	heat source

The previous studies of convective heat transfer deal only with Newtonian fluids. The extension to non-Newtonian fluids is important for the thermal design of industrial equipments dealing with certain fluids, such as ferro liquids, colloidal fluids, animal bloods, and exotic lubricants. The theory of micropolar fluids developed by Eringen [12–14] can be used to describe successfully the non-Newtonian behavior of the above fluids. In the theory, the local effects arising from microstructure and intrinsic motions of the fluid elements are taken into account. Jena and Bhattacharyya [15] proposed the effect of microstructure on thermal convection in a rectangular box heated from below using the Galerkin method, whereby obtained critical Rayleigh numbers for various material parameters. They concluded that the critical Rayleigh number of a micropolar fluid is higher than that of a Newtonian fluid. Recently, Hsu and Chen [16] studied the natural convection of micropolar fluids in a rectangular enclosure heated from below. They indicated that the heat transfer coefficient is lower for a micropolar fluid in comparison with a Newtonian fluid. Furthermore, Hsu and Tsai [17] investigated natural convection of micropolar fluids in an enclosure with a partition. In Ref. [17], the effects of vortex viscosity and spin gradient viscosity on heat transfer coefficient and microrotation were analyzed numerically.

The purpose of this paper is to investigate the effect of the characteristic parameters of micropolar fluids on mixed convection in a cavity. The phenomena of both flow and thermal fields are displayed for effective comparison as well.

2. Mathematical formulation

Consider a square cavity with a finite-length constant-flux heat source embedded on the left vertical wall; the inflow opening located on the left vertical wall; and the outflow opening on the opposite vertical wall. Details of the geometry and coordinate system are shown in Fig. 1. The depth of the cavity is presumed to be long enough so that the whole model is two-dimensional. For simplicity, the two openings are set equal to the height of the heat source. The walls of the cavity are taken as adiabatic. The flow velocities of the fluid through the inflow opening are assumed to be uniform.

The flow is assumed to be steady, laminar, and incompressible. The variation of density with temperature follows the Boussinesq approximation. The governing equations for micropolar fluids in a cavity can be described in dimensionless form by

$$\nabla^2 \Psi = -\Omega \tag{1}$$

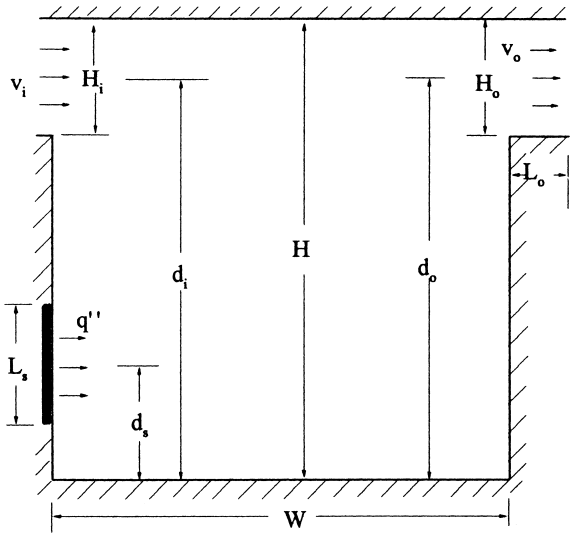

Fig. 1. Physical model of the cavity.

$$U\frac{\partial \Omega}{\partial X}+V\frac{\partial \Omega}{\partial Y}=\frac{1+\Delta}{Re}\nabla^2\Omega-\frac{\Delta}{Re}\nabla^2\upsilon+\eta\frac{\partial\theta}{\partial X} \tag{2}$$

$$U\frac{\partial \upsilon}{\partial X}+V\frac{\partial \upsilon}{\partial Y}=\frac{\Delta B}{Re}(\Omega-2\upsilon)+\frac{\lambda}{Re}\nabla^2\upsilon \tag{3}$$

$$U\frac{\partial \theta}{\partial X}+V\frac{\partial \theta}{\partial Y}=\frac{1}{Pr\times Re}\nabla^2\theta \tag{4}$$

where

$$U=\frac{\partial \Psi}{\partial Y},\quad V=-\frac{\partial \Psi}{\partial X}$$

The above equations are generalized by using the following dimensionless variables

$$X=\frac{x}{A},\quad Y=\frac{y}{A},\quad U=\frac{u}{v_i},\quad V=\frac{v}{v_i},$$

$$\Psi=\frac{\psi}{v_iA},\quad \Omega=\frac{\omega A}{\upsilon_i},\quad \upsilon=\frac{\sigma A}{v_i},\quad \theta=\frac{T-T_i}{\Delta T}$$

where the characteristic length A is the height of the inflow opening.

For the boundary conditions, the vertical and the horizontal solid walls are impermeable ($U = V = 0$) except for the inflow and outflow openings. A uniform inlet velocity profile ($U = 1$, $V = 0$) is taken across the inflow opening. The no-slip conditions at the walls ($U = V = 0$) state that the stream function Ψ is constant at the walls. Thus, $\Psi = 0$ can be arbitrarily chosen for the bottom horizontal wall and both vertical walls that lie below the two openings. While at the top surface, $\Psi = 1$ is specified, since the non-dimensional flow rate is equal to 1. Therefore, by the definition of stream function, a linear variation of the form $\Psi = Y +$ constant is applied for the stream function at the inflow opening.

A third-order polynomial interpolation for the vorticity near the walls is used and is written as

$$\Omega_w=\frac{7\Psi_w-8\Psi_{w+1}+\Psi_{w+2}}{2(\Delta n)^2}+o(\Delta n^2) \tag{5}$$

where n is the direction normal to the wall. At the inflow opening, $\Omega = 0$ is chosen since constant velocity condition ($U = 1$, $V = 0$) is specified.

For the microrotation, the following boundary conditions are assumed at the solid walls,

$$\upsilon=\zeta\frac{\partial V}{\partial X}\quad \text{at } X=0,\,1 \tag{6a}$$

$$\upsilon=-\zeta\frac{\partial U}{\partial Y}\quad \text{at } Y=0,\,1 \tag{6b}$$

where ζ is a constant and $0\le\zeta\le1$. The case $\zeta = 0$, which indicates $\upsilon = 0$, represents concentrated particle flows in which the microelements close to the wall surface are unable to rotate [18]. The case $\zeta = 0.5$ indicates the vanishing of antisymmetric part of the stress tensor and denotes weak concentrations [19]. The case $\zeta = 1$, as suggested by Peddieson [20], is used for the modelling of turbulent boundary layer flows. The case of $\zeta = 0$ is considered in the present study due to the paper limitation.

At the inflow opening, the temperature condition is $\theta = 0$. The condition $\partial\theta/\partial n = 0$ is considered for all adiabatic walls, while $\partial\theta/\partial X = -1$ is for the heat source surface. At the outflow the gradients of all functions have been taken equal to zero, as used in many previous studies [6,10,11]. In order to achieve this adequate condition, a channel of dimensionless length with 1/8 of the width of the cavity is imposed at the outlet opening, as is applied in Ref. [10].

The mean Nusselt number is given by

$$\overline{Nu}=\frac{1}{kL_s}\int_0^{L_s}\frac{q''A}{T_s(y)T_i}\,dy=\int_0^1\frac{1}{\theta_s(Y)}\,dY \tag{7}$$

Here L_s is set equal to A.

3. Numerical scheme

The computational procedure is similar to the one described by Hsu et al. [11] and Rubin and Graves [21]. The resulting system of the coupled Eqs. (1)–(4) with the associated boundary conditions are solved simultaneously by cubic spline approximation method.

The spline alternating direction implicit procedure is adopted to perform the numerical computation. Test for the accuracy of grid fineness is made for the arrangement of 41 × 45 and 81 × 91. It is found that the employment of a 41 × 45 non-uniform grid arrangement can provide sufficiently accurate numerical solutions. The 81 × 91 non-uniform nodes are adopted only at large *Re* numbers.

Employing the false transient technique, the governing Eqs. (1)–(4) are transformed into the following form:

$$\varphi_{ij}^{p+\frac{1}{2}} = F_{ij}^{p} + G_{ij}^{p} m_{\varphi_{ij}}^{p+\frac{1}{2}} + S_{ij}^{p} M_{\varphi_{ij}}^{p+\frac{1}{2}} \tag{8}$$

$$\varphi_{ij}^{p+1} = F_{ij}^{p+\frac{1}{2}} + G_{ij}^{p+\frac{1}{2}} l_{\varphi_{ij}}^{p+1} + S_{ij}^{p+\frac{1}{2}} L_{\varphi_{ij}}^{p+1} \tag{9}$$

in which i and j refer to the computational nodes, p is

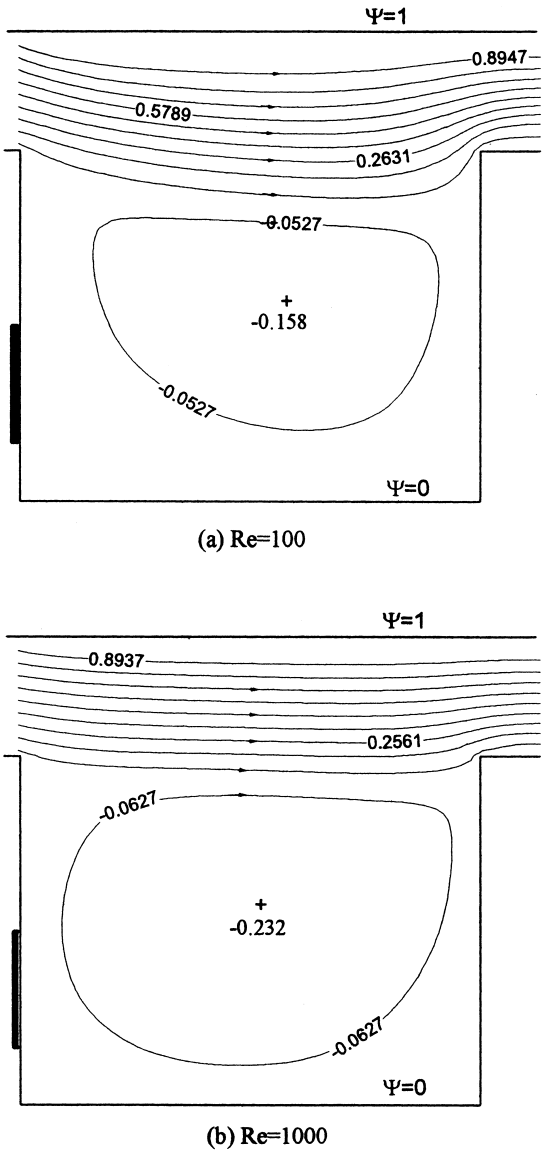

Fig. 2. Streamlines for $\eta = 1$, $B = 0.1$, and $\Delta = \lambda = 1$. (a) $Re = 100$; (b) $Re = 1000$.

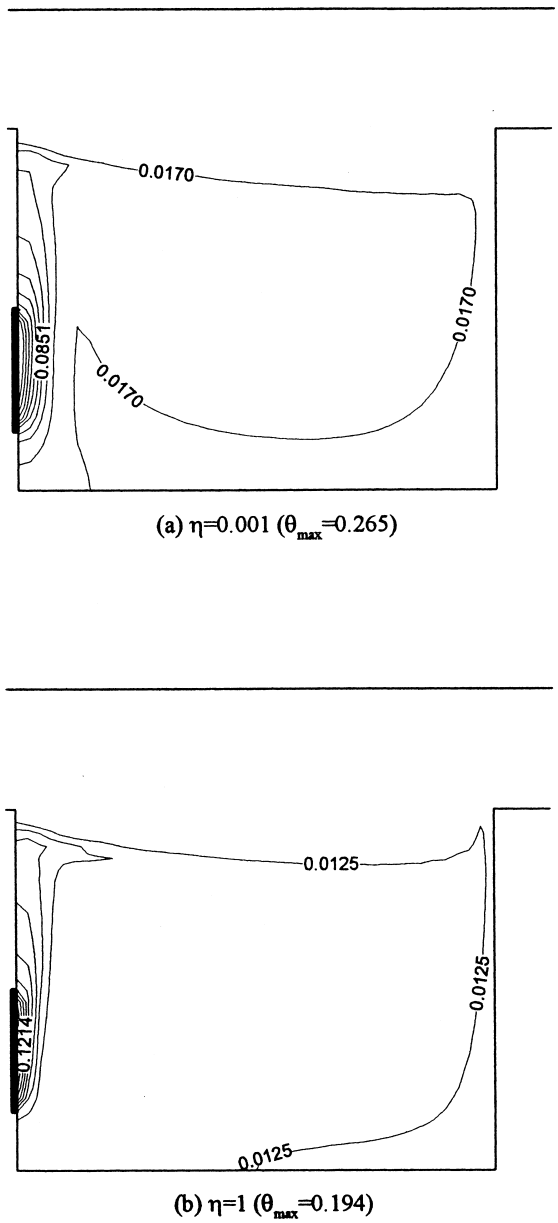

Fig. 3. Maximum source temperatures for $B = 0.1$ and $\Delta = \lambda = 1$.

the false time step, φ represents for the function Ψ, Ω, ν and θ, m, l, M and L are the first and second derivatives of φ with respect to X and Y, respectively, and F_{ij}, G_{ij}, and S_{ij} are the function coefficients calculated at the previous time step.

After transforming by cubic spline collocation method, Eqs. (8) and (9) are rewritten in tridiagonal system containing with the function values or its first two derivatives, that is,

$$A_{j-1}\Phi_{ij-1}^{p+\frac{1}{2}} + B_j\Phi_{ij}^{p+\frac{1}{2}} + C_{j+1}\Phi_{ij+1}^{p+\frac{1}{2}} = D_j \tag{10}$$

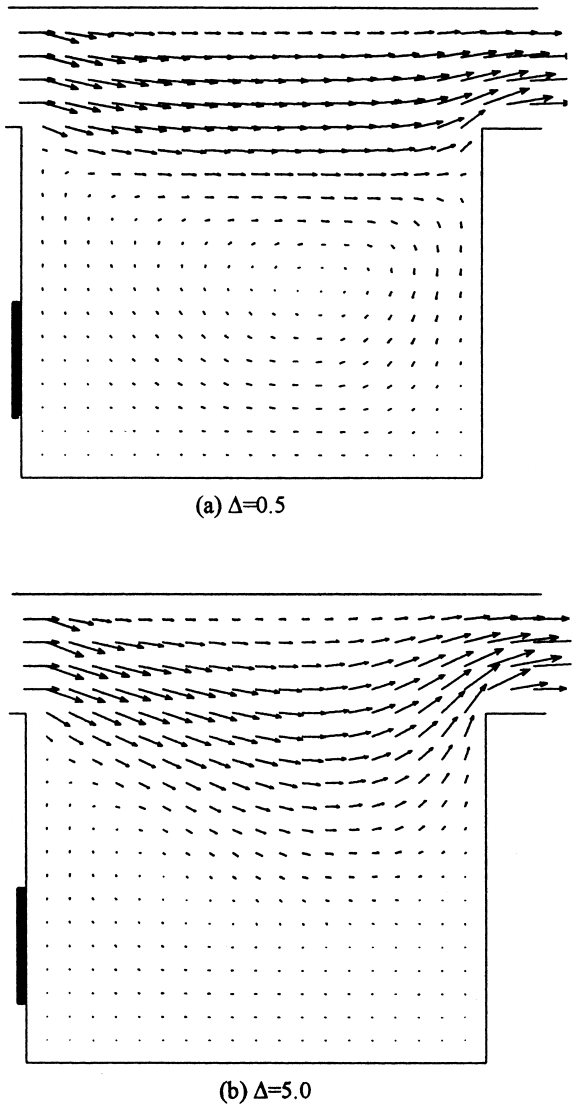

Fig. 4. Isotherms for $Re = 100$, $B = 0.1$, and $\Delta = \lambda = 1$. (a) $\eta = 0.001$ ($\theta_{max} = 0.265$); (b) $\eta = 1$ ($\theta_{max} = 0.194$)

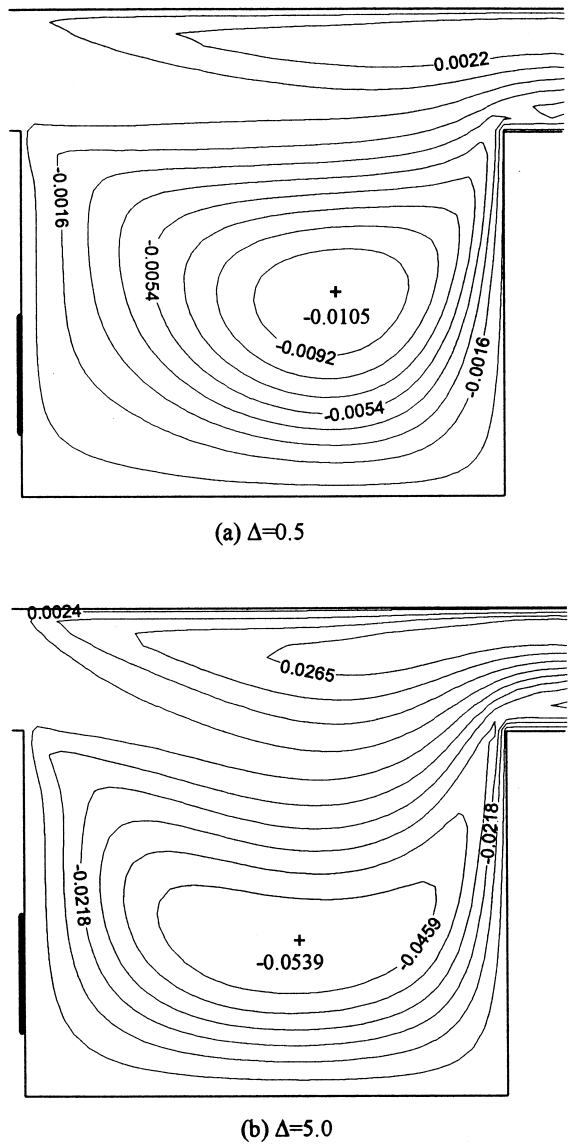

Fig. 5. Velicity vectors for $Re = 100$, $\eta = 1$, $B = 0.1$, and $\lambda = 1$. (a) $\Delta = 0.5$; (b) $\Delta = 5.0$.

$$A_{i-1}\Phi_{i-1,j}^{p+1} + B_i\Phi_{ij}^{p+1} + C_{i+1}\Phi_{i+1,j}^{p+1} = D_i \tag{11}$$

where Φ represents the functions Ψ, Ω, υ and θ or its first two derivatives. Thus, Eqs. (10) and (11) can be easily solved by the Thomas algorithm.

The solution procedures for the coupled Eqs. (1)–(4) are iterated until the maximum relative change in all the flow functions in the cavity satisfies the following convergence condition

$$\left|\frac{\Phi_{ij}^{z} - \Phi_{ij}^{z-1}}{\Phi_{\max}^{z}}\right| \leq 10^{-4} \tag{12}$$

Table 1
Comparison of some results of validity ($Pr = 0.733$)[a]

Re	η	$\overline{Nu}$		θ_{max}	
		Ref. [8]	Present	Ref. [8]	Present
100	0.1	1.45	1.53	0.7	0.60
100	1	2.30	2.50	0.48	0.43
1000	0.1	2.20	2.44	0.52	0.48
1000	1	3.75	3.89	0.30	0.27

[a] Values of Ref. [8] were approximately read.

where Φ refers to Ψ, Ω, υ and θ and z denotes the number of iteration.

The mathematical computation was validated by checking the solutions against those by Papanicolaou and Jaluria [8], which studied mixed convection in a rectangular enclosure with air flowing through the openings. The comparison was shown in Table 1 for various Re and η values. It is seen that the present solutions obtained by similar simulation fairly agree with the predicted results in Ref. [8].

4. Results and discussion

The numerical simulation was performed with $Pr = 10$. The governing parameters considered in the problem were Re, Gr, and various material parameters characterized by micropolar fluids. All these parameters were varied over wide ranges to investigate their effects on the thermal and flow phenomena. The geometric model depicted in Fig. 1 was specified as follows: $H/W = 1$, $A/H = 0.25$, and $L_s = A$. The two openings were fixed at $d_i/H = d_o/H = 0.875$. The values of governing parameters Re and η were $Re = 50$–1000 and $\eta = 0.001$–10. The values chosen for Re were in the laminar regime. Solutions of periodic oscillation behavior were obtained for greater values of η, i.e., $\eta > 10$. The same oscillatory phenomenon mentioned above was also predicted in Ref. [8] for Newtonian fluids. The material parameters for micropolar fluids considered were $B = 0.1$, $\Delta = 0.1$–10 and $\lambda = 0.1$–10. These parameter values satisfy the thermodynamic restriction noted by Eringen [14].

The computed streamlines for the solutions at various values of Re while keeping η fixed are shown in Fig. 2. The first observation in these figures is that the streamlines are almost straight at large Re, and the amount of the recirculation due to boundary increases as Re increases. Therefore, the greater shear force induced by fluid flow at larger Re value causes stronger recirculation and enhances the heat transfer in the cavity, as is shown in Fig. 3 later. The effect of $\eta (= Gr/Re^2)$ on the isotherms is shown in Fig. 4 while keeping Re fixed. Clearly the temperature gradients at the heat source and the heating of the central region of the cavity increase as η increases.

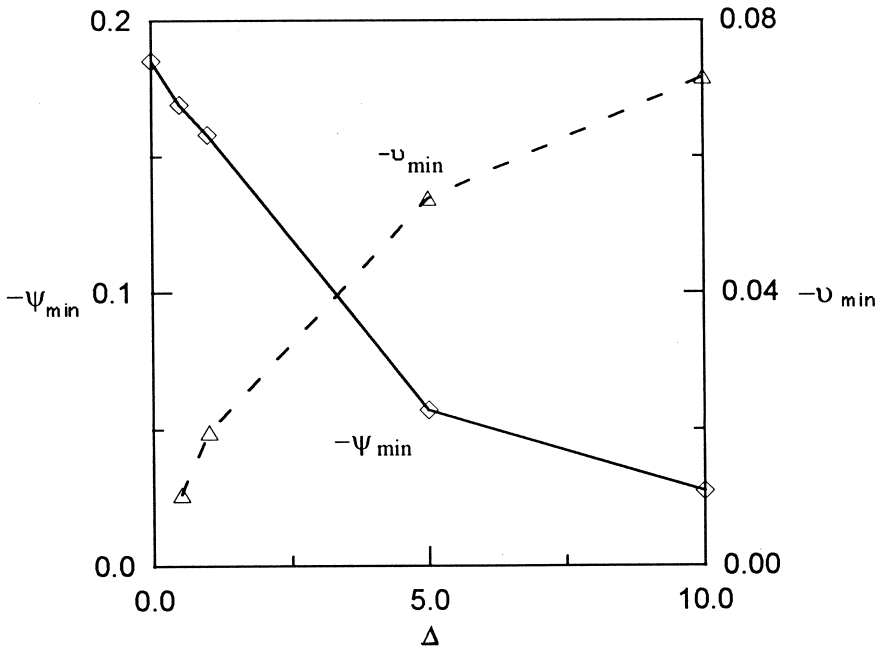

Fig. 6. Microrotation contours for $Re = 100$, $\eta = 1$, $B = 0.1$, and $\lambda = 1$. (a) $\Delta = 0.5$; (b) $\Delta = 5.0$.

Representative velocity vector distributions for various parameters Δ are plotted in Fig. 5 with $Re = 100$, and $\eta = \lambda = 1$. From the figure, it is seen that weak (or even no) recirculation flow due to boundary is present in the cavity. The primary cause of this behavior is that greater value of vortex viscosity Δ corresponds to larger resistance to the fluid motion, which then diminishes the recirculating flow.

The corresponding microrotation distributions in the cavity are shown in Fig. 6 for two values of Δ. An increase in the value of Δ implies a higher vortex viscosity of fluid which promotes the microrotation of micropolar fluids. The effects of the material parameter Δ on both the stream function and microrotation can be explained in Fig. 7. It reveals that an increase in the value of Δ reduces the stream function but enhances the microrotation in the recirculation cell. A greater value of stream function for a Newtonian fluid (i.e., $B = \Delta = \lambda = 0$) is also depicted in the figure. It is concluded that a Newtonian fluid has stronger recirculation flow than a micropolar fluid.

It is interesting to investigate the influence of spin gradient parameter λ on the flow field. Fig. 8 displays the distributions of microrotation in the cavity for various values of λ. The gross amounts of microrotation distribution are smaller for greater value of λ. A further explanation for the effect of parameter λ on the flow characteristics is shown in Fig. 9. In this figure, both stream function and microrotation, that are the values at the recirculation core, are plotted against the parameter λ. It is found that the microrotation at the recirculation cell decreases as the spin gradient viscosity λ increases. However, except at small value of λ, no significant variation of stream function at the recirculation cell occurs for $\lambda > 1$. One may also notice how the stream function at recirculation core gradually increase with decreasing value of λ, until it reaches the maximum amount of $\lambda = 0$ (and $B = \Delta = 0$), which is specifically a Newtonian fluid.

Fig. 10 shows a very illustrative picture of how the heat is transferred in accordance with Re and η. Keeping Re constant, the average Nusselt number increases gradually with increasing value of η. Also, the average Nusselt number is found to increase as Re increases at fixed η. Therefore, it can be concluded that more heat transfer from the heat source is expected in the case of large parameter value of Re or η. The dashed lines in the figure indicate the variation of average Nusselt number corresponding to the case of a Newtonian fluid. At the same values of Re and η, the average Nusselt number for a Newtonian fluid is higher than the case for a micropolar fluid, especially at large Re value. It is a fact that both the vortex viscosity parameter and spin gradient viscosity parameter λ retard the fluid motion in the cavity. Smaller values of stream function for micropolar fluids at the recirculation cell are obtained, as are shown in Figs. 6 and 8. This fact explains the results of lower average Nusselt number for a micropolar fluid in Fig. 9.

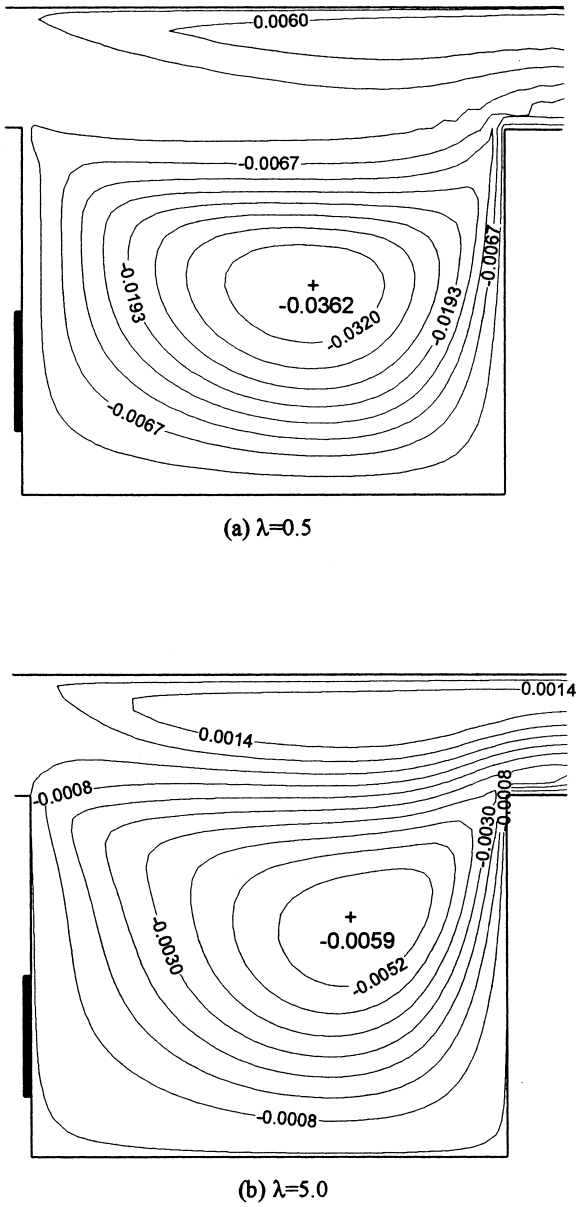

Fig. 7. Maximum values of recirculation stream funcion and microrotation for $Re = 100$, $B = 0.1$, and $\eta = \lambda = 1$.

Fig. 11 displays the dependence of average heat transfer coefficient and the maximum surface temperature on the material parameter Δ. As pointed in Fig. 6, an increase in Δ results in a decrease in stream function at the recirculation core. Therefore, less heat transfer rate from the heat source is achieved due to

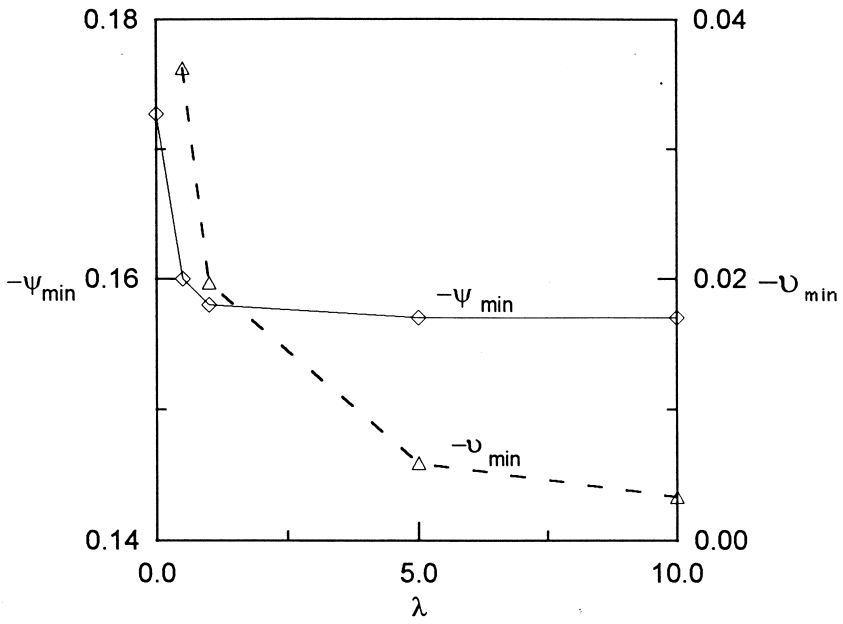

Fig. 8. Microrotation contours for $Re = 100$, $\eta = 1$, $B = 0.1$, and $\Delta = 1$. (a) $\lambda = 0.5$; (b) $\lambda = 5.0$.

decreased recirculating flow. In addition, the lower heat transfer rate accompanies with a higher temperature on the source surface, which is also shown in Fig. 11.

Some quantitative numerical results are tabulated in Table 2. The computational values indicate that increasing the value of Δ leads to a decrease in the values of the average Nusselt number. Whereas, the variation of λ has almost no influence on the average Nusselt number. The numerical value of the microrotation depends to a large extent on both the values of Δ and λ. An increased microrotation can be obtained by increasing the value of Δ or by reducing the value of λ.

Table 2
Comparison of selected results for $Pr = 10$ and $B = 0.1$ [a]

Re	η	Δ	λ	$\overline{Nu}$	Ψ_{min}	θ_{max}	ν_{min}
50	1	1	1	3.3433	−0.0673	0.2724	−0.0214
100	1	0	0	5.2544	−0.1854	0.1727	–
100	1	0.5	0.5	5.0311	−0.1722	0.1809	−0.0203
100	0.01	1	1	3.31193	−0.1443	0.2621	−0.0197
100	1	1	1	4.7132	−0.1583	0.1940	−0.0197
100	10	1	1	6.8322	−0.2022	0.1327	−0.0232
100	1	5	1	3.8653	−0.0572	0.2331	−0.0539
100	1	10	1	3.2844	−0.0273	0.2739	−0.0717
100	1	1	5	4.7552	−0.1574	0.1917	−0.0059
100	1	1	10	4.7549	−0.1571	0.1917	−0.0034
100	1	5	5	3.6781	−0.0449	0.2456	−0.0225
500	1	0	0	11.500	−0.2264	0.0757	–
500	1	1	1	10.249	−0.2211	0.0871	−0.0221
1000	1	1	1	14.543	−0.2322	0.0594	−0.0253

[a] $B = \Delta = \lambda = 0$: Newtonian fluids.

5. Conclusion

Mixed convection of micropolar fluids in a cavity

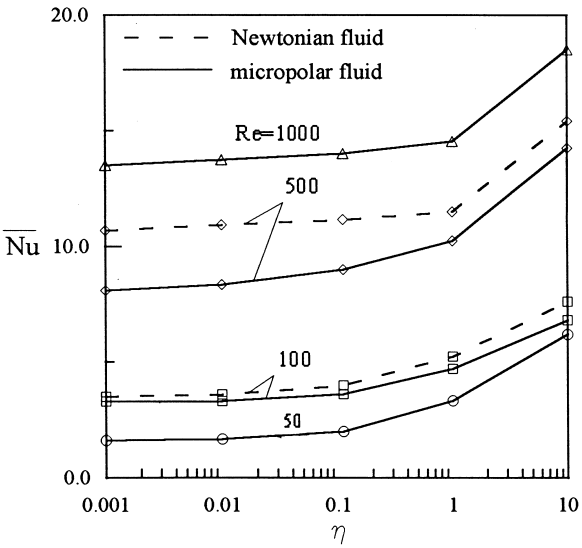

Fig. 9. Maximum values of recirculation stream function and microrotation for $Re = 100$, $B = 0.1$, and $\eta = \Delta = 1$.

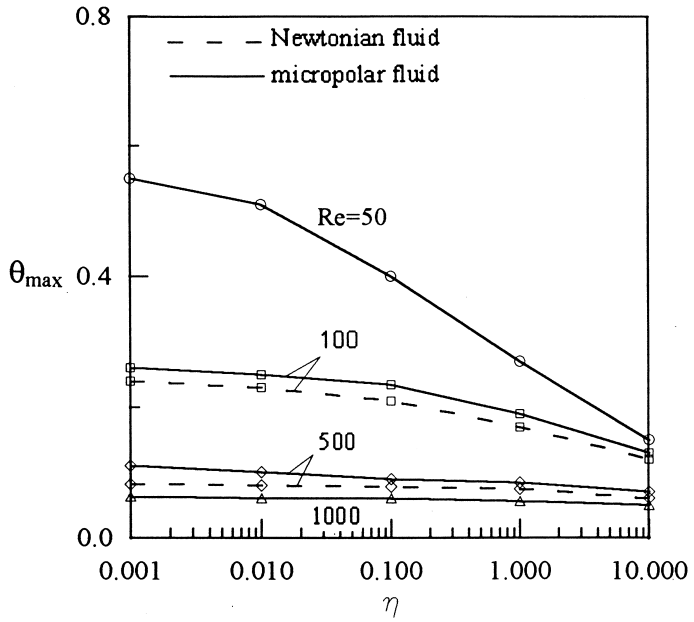

Fig. 10. Average Nusselt numbers for $B = 0.1$ and $\Delta = \lambda = 1$.

with an isolated heat source has been analyzed numerically. Both the thermal and flow fields in the cavity are also computed for a Newtonian fluid for comparison reason. Of interests are the effects of governing parameters (Re and Gr) and material parameters (Δ and λ) on the flow fields and the average Nusselt number.

The numerical solutions indicate that increasing the amount of Re or Gr leads to higher heat transfer coefficient, higher heat source temperature, and higher value of recirculation. The heat transfer coefficient is lower for a micropolar fluid, as compared to a Newtonian fluid.

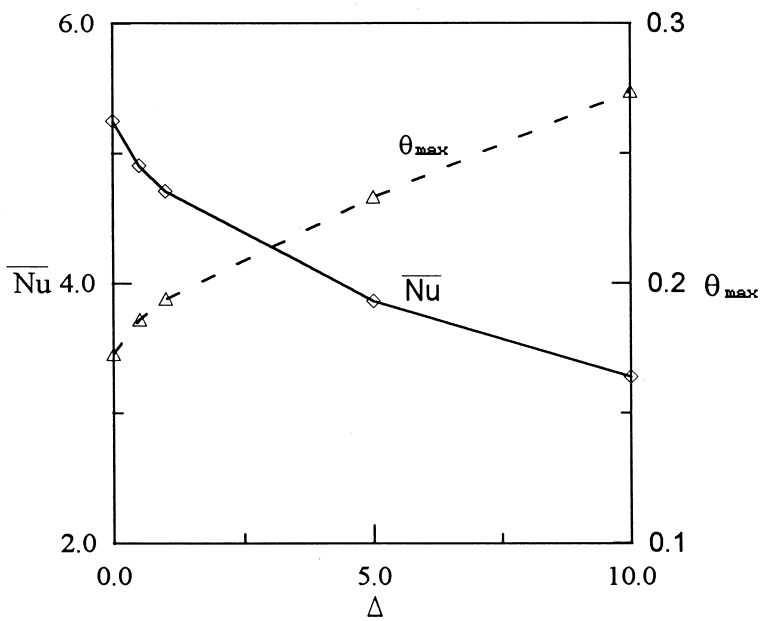

Fig. 11. Average Nusselt numbers and maximum source temperatures for $Re = 100$, $B = 0.1$, and $\eta = \lambda = 1$.

The results performed show a very significant effect of microstructure on the thermal and flow fields. Considerable effects on both thermal and flow fields are found for variation of vortex viscosity, but are little by spin gradient viscosity. The amount of microrotation in the cavity increases when vortex viscosity increases. However, its value becomes lower as spin gradient viscosity is higher.

Acknowledgements

This work was supported by the National Science Council in Taiwan under grant No. NSC-87-2212-E-151-007.

References

[1] G. de Vahl Davis, I.P. Jones, Natural convection in a square cavity: a comparison exercise, Int. J. Numer. Methods Fluids 3 (1983) 227–248.
[2] E. Penot, Numerical calculation of two-dimensional natural convection in isothermal open cavities, Numer. Heat Transfer 5 (1982) 421–437.
[3] S.W. Churchill, C.V.S. Patterson, H.H.S. Chu, The effect of heater size, location, aspect ratio, and boundary conditions on two-dimensional, laminar, natural convection in a rectangular enclosure, J. Heat Transfer 98 (2) (1976) 194–201.
[4] G.P. Paterson, A. Ortega, Thermal control of electronic equipments and devices, Adv. Heat Transfer 20 (1990) 181–314.
[5] K.J. Kennedy, A. Zebib, Combined free and forced convection between horizontal parallel plates, Int. J. Heat Mass Transfer 26 (3) (1983) 471–474.
[6] C.Y. Choi, A. Ortega, Mixed convection in an inclined channel with a discrete heat source, Int. J. Heat Mass Transfer 36 (2) (1993) 3119–3134.
[7] C. Yucel, H. Hasnaoui, L. Robillard, E. Bilgen, Mixed convection heat transfer in open ended inclined channels with discrete isothermal heating, Numer. Heat Transfer Part A 24 (1993) 109–126.
[8] E. Papanicolaou, Y. Jaluria, Mixed convection from an isolated heat source in a rectangular enclosure, Numer. Heat Transfer Part A 18 (1990) 427–461.
[9] E. Papanicolaou, Y. Jaluria, Mixed convection from a localized heat source in a cavity with conducting walls: a numerical study, Numer. Heat Transfer Part A 23 (1993) 463–484.
[10] E. Papanicolaou, Y. Jaluria, Computation of turbulent flow in mixed convection in a cavity with a localized heat source, ASME J. Heat Transfer 17 (1995) 649–658.
[11] T.H. Hsu, P.T. Hsu, S.P. How, Mixed convection in a partially divided rectangular enclosure, Numer. Heat Transfer Part A 31 (1997) 655–683.
[12] A.C. Eringen, Simple microfluids, Int. J. Engng. Sci 2 (1964) 205–217.
[13] A.C. Eringen, Theory of micropolar fluids, J. Math. Mech 16 (1966) 1–18.
[14] A.C. Eringen, Theory of thermomicrofluids, J. Math. Analysis Applic 38 (1972) 480–496.
[15] S.K. Jena, S.P. Bhatacharyya, The effect of microstructure on the thermal convection in a rectangular box of fluid heated from below, Int. J. Engng. Sci 24 (1986) 67–76.
[16] T.H. Hsu, C.K. Chen, Natural convection of micropolar fluids in a rectangular enclosure, Int. J. Engng. Sci 34 (4) (1996) 407–415.
[17] T.H. Hsu, S.Y. Tsai, Natural convection of micropolar fluids in a two-dimensional enclosure with a conductive partition, Numer. Heat Transfer Part A 28 (1995) 69–83.
[18] S.K. Jena, M.N. Mathur, Similarity solutions for laminar free convection flow of a thermomicropolar fluids past a nonisothermal vertical flat plate, Int. J. Engng. Sci 19 (1991) 1431–1439.
[19] G. Ahmadi, Self-similar solutions of incompressible micropolar boundary layer flow over a semi-infinite plate, Int. J. Engng. Sci 14 (1976) 639–646.
[20] J. Peddieson, An application of the micropolar fluid model to the calculation of turbulent shear flow, Int. J. Engng. Sci 10 (1972) 23–32.
[21] S.G. Rubin, R.A. Graves, Viscous flow solution with a cubic spline approximation, Computers and Fluids 1 (1975) 1–36.